Key Engineering Materials
ISSN: 1662-9795, Vol. 926, pp 2129-2136
doi:10.4028/p-abe455

Submitted: 2021-12-01
Revised: 2022-01-27
Accepted: 2022-01-28
Online: 2022-07-22

Error Estimation of the 3D Reconstruction of a Displacement Field from DIC Measurements

Miguel G. Oliveira[1,2,a*], Attilio Lattanzi[3,b], Sandrine Thuillier[2,c], António Andrade-Campos[1,d], and Marco Rossi[3,e]

[1]Centre for Mechanical Technology and Automation (TEMA), Department of Mechanical Engineering, University of Aveiro, 3810-193 Aveiro, Portugal

[2]Univ. Bretagne Sud, UMR CNRS 6027, IRDL, F-56100 Lorient, France

[3]Department of Industrial Engineering and Mathematical Sciences, Università Politecnica delle Marche, 60131 Ancona, Italy

[a]oliveiramiguel@ua.pt, [b]a.lattanzi@staff.univpm.it, [c]sandrine.thuillier@univ-ubs.fr, [d]gilac@ua.pt, [e]m.rossi@staff.univpm.it

Keywords: Volume Reconstruction, Digital Image Correlation, Virtual Experiments, Error Estimation.

Abstract. To enable an accurate simulation of manufacturing processes, it is essential to characterise and model the mechanical behaviour of metallic parts up to large deformations. However, after the onset of necking, deformation becomes highly heterogeneous and the stress is triaxial. By combining full-field measurements and inverse methods, it is possible to calibrate the mechanical behaviour beyond necking. A possibility is to use the virtual fields method, by extending its formulation to a fully three-dimensional approach. However, measuring deformation in the bulk of the material is still a challenge. To address this limitation, a volume reconstruction method able to estimate the deformation inside the specimen was proposed and successfully validated. The aim of this work is to estimate the error of the volume reconstruction method by using a simulated tensile test and the measurement chain associated with a virtual stereo-DIC setup composed of four cameras. A three-dimensional finite element model is used to deform synthetically generated images. The DIC field maps obtained with different setup configurations and DIC settings are used to estimate the error by comparing the reconstructed volume with the reference finite element model. Results show that the impact of conditions and DIC settings on the reconstructed volume is low.

Introduction

From a macroscopic point of view, it is essential to characterise and model the mechanical behaviour of metallic parts up to large deformations, enabling an accurate simulation of manufacturing processes. However, the occurrence of plastic instabilities at large deformations, such as diffuse and localised necking [1, 2], introduces additional challenges to the constitutive modelling. Necking makes the deformation non-uniform and the stress state inside the specimen triaxial, eventually leading to fracture. Besides, plastic deformation becomes highly heterogeneous and concentrates within the necking region. A classical method to characterize the mechanical behaviour is to use the information up to necking, but it can limit the strain range drastically. Alternatively, by combining full-field measurements with inverse methods, it is possible to calibrate a constitutive model beyond necking where deformation is no longer homogeneous, such as using the finite element model updating (FEMU) method [3]. The virtual fields method (VFM) can potentially be used as an alternative to FEMU, but so far it has been mainly used in the two-dimensional space where plane stress conditions are assumed, and therefore exploiting data beyond necking is not obvious. However, because the stress is triaxial, using the virtual fields method considering plane stress assumptions is no longer valid, and a three-dimensional (3D) analysis is required [4, 5].

In material testing and characterisation, the adoption of full-field optical techniques is increasingly becoming the standard procedure [6]. The advantage of these techniques is the measurement of displacement and strain fields on the specimens' surface of complex shapes. It enables the transition from

classical mechanical tests to more complex ones, leading to more data acquisition from a single test. Consequently, it reduces the cost and effort of material testing and improves the accuracy of calibrated constitutive models.

Among full-field optical techniques, digital image correlation (DIC) is the most widespread and fast-growing method [7]. The most common optical setup nowadays is a two-camera setup that can acquire the surface displacements in the 3D space (Stereo-DIC). However, using DIC to obtain information in the bulk of the material is still a big challenge [8]. In the lack of bulk measurements, plane stress conditions can be assumed to estimate the deformation in the thickness direction. While technology is still limited to surface displacements, efforts have been made to, at least, reconstruct the 3D displacement field over the whole external surface of solids [9–11].

Starting from surface full-field measurements, a volume reconstruction method, named internal mesh generation, able to reconstruct the volume displacement field of a solid was introduced [12]. The proposed method can potentially replace more advanced and costly techniques, and its feasibility was already validated by numerical and experimental results. However, in-depth uncertainty quantification of the method has not yet been performed.

The final aim of using the internal mesh generation method is to accurately reconstruct the strain field over the whole volume of a specimen. To achieve that, first this work aims to estimate the error of the volume reconstruction method by using synthetically generated images that mimic real experiments. These synthetic images are generated from displacement fields obtained from a finite element analysis, which are then used to deform a random speckle pattern of the specimen configuration [13]. The interest in using synthetic images is to reduce the gap to experimentally acquired measurements without having to perform the real experiment.

Internal Mesh Generation Method

The internal mesh generation (IMG) method was proposed with the aim of reconstructing the volume displacement field inside a solid by starting from surface measurements [12]. It can be applied to flat or cylindrical specimens, but only the first one is considered here. In the undeformed configuration, flat specimens are assumed to have a constant thickness and two opposite parallel faces. A requirement of the IMG method is that the displacement field is known a priori on both surfaces, named here Surface A and Surface B. A schematic illustration of the measurement points on Surface A and Surface B, both in undeformed and deformed configurations, is shown in Fig. 1. The coordinate system is chosen so that the z-axis is perpendicular to the thickness in the undeformed configuration. Additionally, $\mathbf{N}_\mathrm{A}$ and $\mathbf{N}_\mathrm{B}$ are coordinate vectors representing points in Surface A and Surface B, respectively. $\mathbf{N}_\mathrm{A}$ and $\mathbf{N}_\mathrm{B}$ share the same coordinates in the xy plane, but a different z coordinate.

The IMG method uses quadratic Bézier curves defined by one point on each surface, $\mathbf{N}_\mathrm{A}$ and $\mathbf{N}_\mathrm{B}$, and an internal point $\mathbf{P}$ inside the volume. The resulting Bézier curve $\mathbf{B}(t)$ is defined as

$$\mathbf{B}(t) = (1-t)^2\mathbf{N}_\mathrm{A} + 2(1-t)\mathbf{P} + t^2\mathbf{N}_\mathrm{B}, \tag{1}$$

with $0 \leq t \leq 1$, so that $\mathbf{B}(0) = \mathbf{N}_\mathrm{A}$ and $\mathbf{B}(1) = \mathbf{N}_\mathrm{B}$. Additionally, the Bézier curve is tangent to segment $\overline{\mathbf{N}_\mathrm{A}\mathbf{P}}$ at $\mathbf{B}(0)$ and to segment $\overline{\mathbf{N}_\mathrm{B}\mathbf{P}}$ at $\mathbf{B}(1)$.

The methodology behind the IMG method is schematically illustrated in Fig. 2, for the undeformed and deformed configurations. For the sake of clarity, the point of view is chosen perpendicular to the x-direction, however, points and vectors are considered in the 3D space. The internal point $\mathbf{P}$ is defined as the intersection between the straight line perpendicular to Surface A (or Surface B) in $\mathbf{N}_\mathrm{A}$ (or $\mathbf{N}_\mathrm{B}$) and the mid-plane perpendicular to segment $\overline{\mathbf{N}_\mathrm{A}\mathbf{N}_\mathrm{B}}$. In the undeformed configuration, the internal point $\mathbf{P}$ is simply defined as the average of the surface points $\mathbf{N}_\mathrm{A}$ and $\mathbf{N}_\mathrm{B}$:

$$\mathbf{P} = (\mathbf{N}_\mathrm{A} + \mathbf{N}_\mathrm{B})/2, \tag{2}$$

yielding a straight line from $\mathbf{N}_\mathrm{A}$ to $\mathbf{N}_\mathrm{B}$. However, in the deformed configuration the specimen is not flat anymore and two different internal points $\mathbf{P}_\mathrm{A}$ and $\mathbf{P}_\mathrm{B}$ are obtained by starting from $\mathbf{N}_\mathrm{A}$ and $\mathbf{N}_\mathrm{B}$,

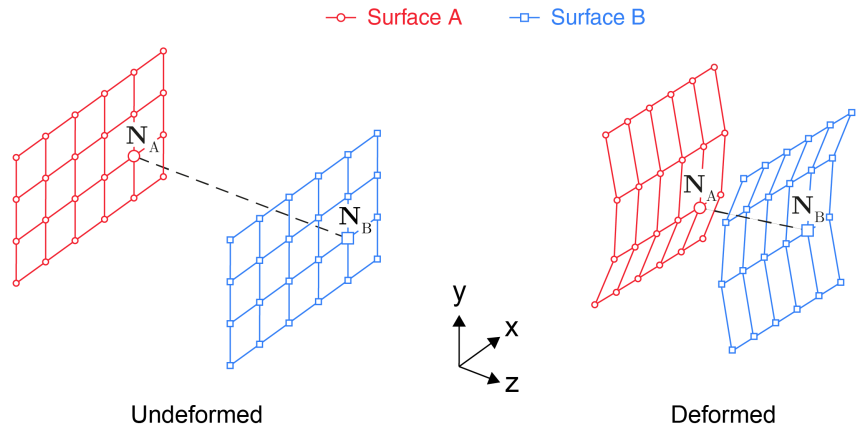

Fig. 1: Schematic illustration of measurement points of surfaces in the (a) undeformed and (b) deformed configurations.

respectively. Then, according to geometrical considerations the internal points $\mathbf{P}_\mathrm{A}$ and $\mathbf{P}_\mathrm{B}$ are defined as

$$\mathbf{P}_\mathrm{A} = \mathbf{N}_\mathrm{A} - \frac{|\mathbf{N}_\mathrm{A} - \mathbf{N}_\mathrm{B}|^2}{2\,(\mathbf{N}_\mathrm{A} - \mathbf{N}_\mathrm{B}) \cdot \hat{\mathbf{n}}_\mathrm{A}} \hat{\mathbf{n}}_\mathrm{A}, \tag{3}$$

$$\mathbf{P}_\mathrm{B} = \mathbf{N}_\mathrm{B} - \frac{|\mathbf{N}_\mathrm{B} - \mathbf{N}_\mathrm{A}|^2}{2\,(\mathbf{N}_\mathrm{B} - \mathbf{N}_\mathrm{A}) \cdot \hat{\mathbf{n}}_\mathrm{B}} \hat{\mathbf{n}}_\mathrm{B}, \tag{4}$$

where $\cdot$ is the scalar product, and $\hat{\mathbf{n}}_\mathrm{A}$ and $\hat{\mathbf{n}}_\mathrm{B}$ are the normals to Surface A and Surface B, respectively, at points $\mathbf{N}_\mathrm{A}$ and $\mathbf{N}_\mathrm{B}$. The internal point $\mathbf{P}$ is then computed as

$$\mathbf{P} = \frac{\mathbf{P}_\mathrm{A} + \mathbf{P}_\mathrm{B}}{2}. \tag{5}$$

It can be pointed out that, if the deformation is symmetrical, as it theoretically occurs in isotropic materials, $\mathbf{P}_\mathrm{A}$, $\mathbf{P}_\mathrm{B}$, and $\mathbf{P}$ will be coincident. However, because of measurement errors and possible anisotropy of heterogeneous materials, the former is not usually true.

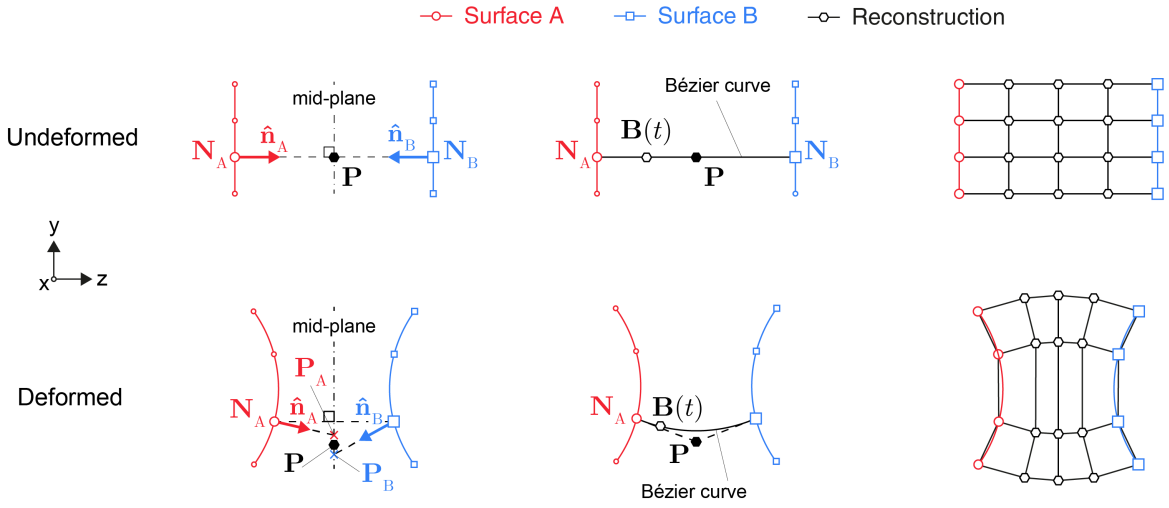

Fig. 2: Schematic of the internal mesh generation method for flat specimens in the (a) undeformed and (b) deformed configurations.

Choosing a suitable number of internal points and repeating this procedure for all the points of the surfaces a 3D mesh is reconstructed. At the end, the volume displacement and strain fields are computed using the shape functions of the hexahedral elements, as illustrated in the last schematic of Fig. 2.

Finite Element Model

To evaluate the accuracy of the IMG method when applied to real experiments, a numerical simulation is used for which the whole volume deformation history is known. The finite element model reproduces the necking evolution in specimens under severe plastic deformation. Here, a 20 mm thick flat specimen is considered, under a plane strain tensile test and an initial rectangular section. The finite element model is 3D and was built up using the commercial software Abaqus. An eight-node brick element with reduced integration is used, as well as a large strain formulation. The global element size is 1 mm and a structured mesh is used in the region-of-interest between 76×20 mm^2 in the xy plane.

The material parameters and constitutive law were chosen to resemble the behaviour of a metal with high anisotropy. The Hill 48 yield criterion is used to describe the yield surface and Swift's power law is selected to describe the stress-strain hardening curve. The input constitutive parameters, including Young's modulus E and Poisson's ratio ν, are provided in Table 1.

Table 1: Material's elastic properties and constitutive parameters used in Hill 48 anisotropic yield criterion and Swift's isotropic hardening law.

Elasticity		Hill 48						Swift		
E [GPa]	ν	F	G	H	N	M	L	σ_0 [MPa]	K [MPa]	n
70	0.3	0.252	0.826	0.174	2.242	1.500	1.500	226.7	310.5	0.08

The undeformed and deformed configurations are shown in Fig. 3 where it is possible to notice that a severe necking occurs at the centre of the specimen. The necking is associated to a complex 3D deformation field as illustrated over the cross-sections of Fig. 3(c). The maximum strain is obtained at the inner part of the specimen and, thus, cannot be directly evaluated by surface measurements. The value of the equivalent strain is about 1, which falls in the range of the fracture strain observed for ductile metals.

Next, the IMG method is used to reconstruct the internal displacement and strain fields and compared to the reference from the finite element analyses.

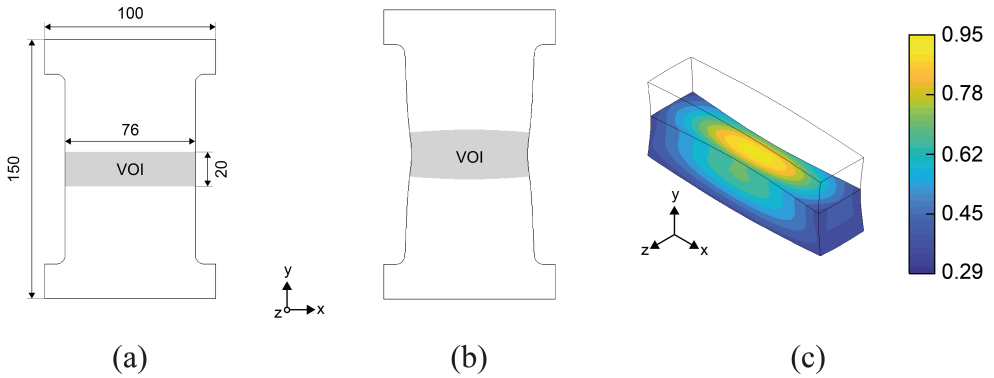

Fig. 3: Finite element model of tensile test in the (a) undeformed configuration, (b) deformed configuration, and (c) 3D view cut of volume of interest (VOI) with the equivalent plastic strain distribution in the deformed configuration. Dimensions in millimetres.

Volume Reconstruction from Stereo-DIC Virtual Experiments

The volume reconstruction error coming from the IMG method itself has been established, however, in real experiments, a large number of experimental conditions will influence the quality of the measurements. To include these conditions in the volume reconstruction, virtual experiments are introduced to evaluate the uncertainty of the IMG method under experimental conditions. In particular, virtual stereo-DIC experiments are used to measure more accurately the out-of-plane displacements. To simulate the measurement chain associated with a virtual stereo-DIC setup, four virtual cameras are used to measure the displacement field in the front and the back of the specimen, two for each surface. Recall that one of the requirements of the IMG method is to start from surface measurements of back-to-back surfaces. The virtual experiments are generated according to the procedure described in [14, 15] to retrieve the displacement fields by deforming a reference speckle pattern. It should be noted that the procedure is performed for both surfaces of the specimen, and it is as follows:

1. Export FEA mesh and 3D displacement field;
2. Impose FEA mesh onto a reference speckle pattern image;
3. Generate synthetically deformed stereo-DIC images;
4. Perform stereo-DIC measurements;
5. Export stereo-DIC measurements to IMG method.

In real experiments using stereo-vision systems, many factors can influence the accuracy of the final measurements. Evaluating the influence of all of them in the volume reconstruction would be a hard and long task. Therefore, a design of experiments is performed by selecting five different factors which can influence the final stereo-DIC measurements and consequently the volume reconstruction. These factors can be introduced along the procedure chain presented above. Another factor is the speckle pattern applied to the specimen. However, to simplify the analysis, an image of a real speckle pattern, is used as reference to generate all virtual experiments, as shown in Fig. 4.

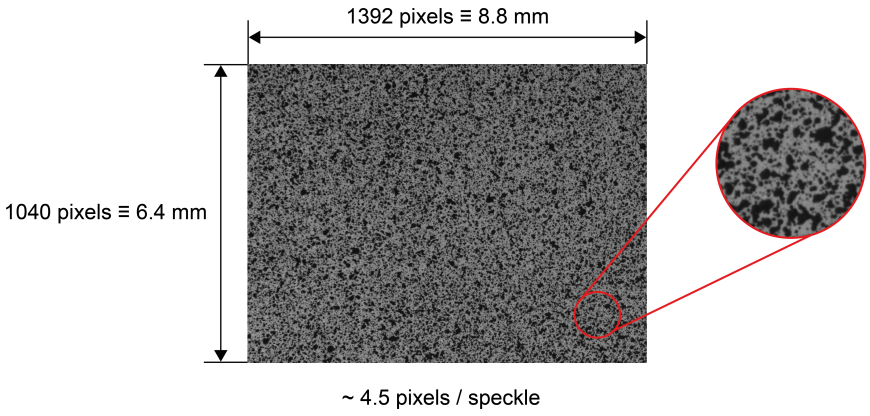

Fig. 4: Image of real speckle pattern used as reference to generate the virtual experiments.

In Table 2 are shown the selected factors, where for each of them, three different levels are evaluated in order to obtain a quadratic response. The design of experiments is composed of 243 virtual experiments in total. It should be noted that the two stereo-angle values in each level correspond to the front and back stereo-vision systems, respectively. The noise values correspond to the standard deviation of a Gaussian distribution for an 8-bit image. MatchID software was used to generate the synthetic images and perform stereo-DIC measurements [16].

Table 2: Factors and levels for the design of experiments to evaluate the volume reconstruction from virtual experiments.

Level	Field of View [mm^2]	Stereo-Angle [°]	Noise [grey level]	Subset Size [px^2]	Step Size [px]
1	76 × 112	15 / 16	0	17	3
2	76 × 148	20 / 21	5	21	5
3	76 × 160	25 / 26	10	25	7

To isolate the influence of introducing virtual experiments in the IMG method, the error is computed as the difference between the reconstruction using FEA and virtual experiments. The results are presented in Figs. 5 and 6, respectively, for the displacement and logarithmic strain components. The presented results analyse the major effects of each factor, allowing a comparison of its influence on the error. Therefore, each level within each factor corresponds to the mean result of 81 experiments. Moreover, for the sake of simplicity, only the mean of error of all the points or elements in the volume of interest (VOI) is represented. It is considered that the mean error can describe on an average way the influence of each factor.

It is observed that an increase in the field-of-view leads to an error increase in all the components of displacement and logarithmic strain. Moreover, it appears that the field of view is the factor with the biggest impact out of the five factors evaluated, as variations between levels are more pronounced. The same pattern can be observed for the noise, even though its impact on the displacement error is low and is more evident in the logarithmic strain. On the other hand, the subset size appears to have a low impact on the error. The impact of stereo-angle is not well understood and some conflicting results are observed. Perhaps the stereo-angle should be analysed in function of lenses focal length, because the choice of lenses will influence the stereo-angle. Overall, the influence of these factors is quantitative low in the obtained error. However, these low variations can also be explained by the range of values selected for each factor. Expanding the range of values can potentially yield different results, but it is not expected that the error will increase drastically.

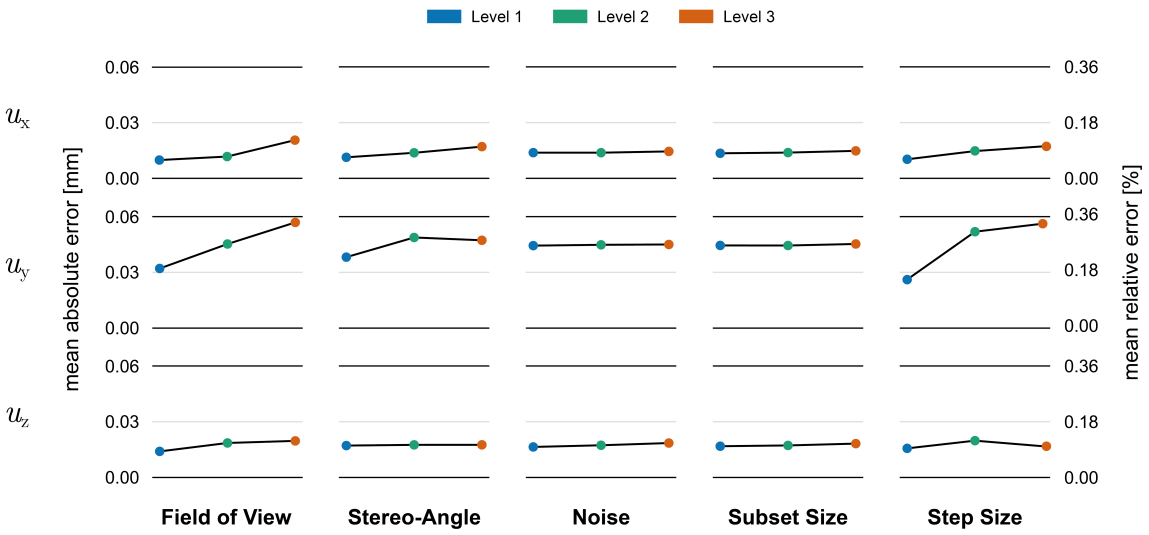

Fig. 5: Mean error between reconstructed volume of interest using finite element analysis and using virtual experiments for the displacement components. Rows corresponds to the displacement components and columns to the factors in the design of experiments.

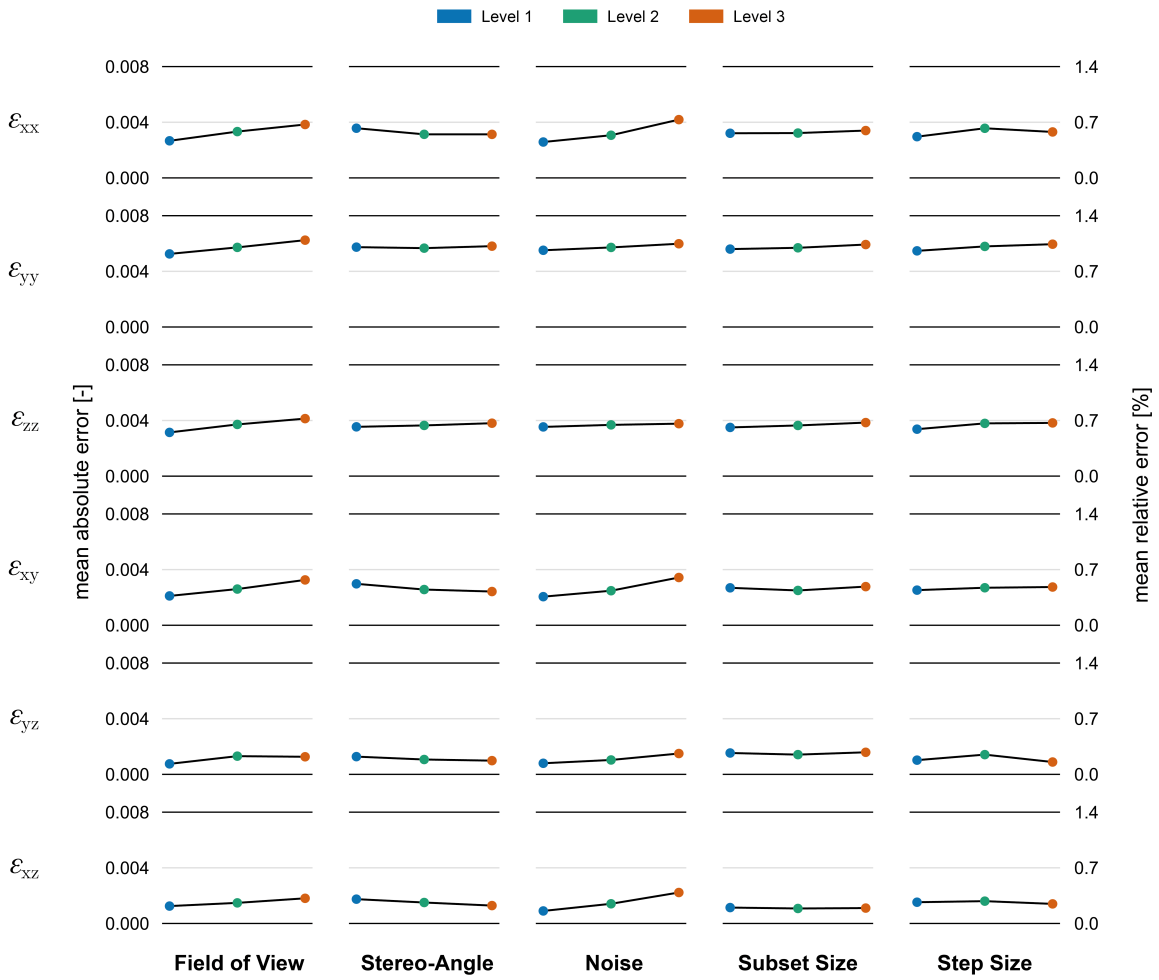

Fig. 6: Mean error between reconstructed volume of interest using finite element analysis and using virtual experiments for the logarithmic strain components. Rows corresponds to the logarithmic strain components and columns to the factors in the design of experiments.

Conclusions

This work estimated the error of a volume reconstruction method, name internal mesh generation, able to estimate the deformation inside a solid. At first, the reconstruction method was applied to surface data extracted from a finite element analysis of a tensile test. Stereo-DIC virtual experiments were successfully applied to estimate the error of the volume reconstruction method. It was observed that the virtual experiments have a low impact on the estimated error. To understand the influence of experimental conditions and DIC settings, a design of experiments considering five different factors with three levels each was performed. It was shown that the field-of-view influences the most the estimated error, but that overall the influence of these factors is relatively low.

Acknowledgments

This project has received funding from the Research Fund for Coal and Steel under grant agreement No. 888153. The authors also gratefully acknowledge the financial support of the Portuguese Foundation for Science and Technology (FCT) under the projects PTDC/EME-APL/29713/2017, PTDC/EME-EME/30592/2017 by UE/FEDER through the programs CENTRO 2020 and COMPETE 2020, and UID/EMS/00481/2013-FCT under CENTRO-01-0145-FEDER-022083. The authors also would like to acknowledge the Région Bretagne for its financial support and BPI France under project

EXPRESSo. Also, this project would not be possible without the financial support of Région Bretagne and ESAFORM to the international mobility action of Miguel G. Oliveira at the Università Politecnica delle Marche. Miguel G. Oliveira is grateful to the FCT for the PhD grant SFRH/BD/143665/2019.

References

[1] A. E. Bayoumi and R. Joshi, "On the formabllity/instability of stretch-forming sheet metals," *Applied Mechanics Reviews*, vol. 45, S154–S164, 3S 1992.

[2] R. Hill, "On the mechanics of localized necking in anisotropic sheet metals," *Journal of the Mechanics and Physics of Solids*, vol. 49, pp. 2055–2070, 2001.

[3] A. Pradeau, S. Thuillier, and J. W. Yoon, "Prediction of failure in bending of an aluminium sheet alloy," *International Journal of Mechanical Sciences*, vol. 119, pp. 23–35, 2016.

[4] M. Rossi and F. Pierron, "Identification of the plastic behaviour in the post-necking regime using a three dimensional reconstruction technique," vol. 504-506, Trans Tech Publications Ltd, 2012, pp. 703–708.

[5] J. H. Kim, A. Serpantié, F. Barlat, F. Pierron, and M. G. Lee, "Characterization of the post-necking strain hardening behavior using the virtual fields method," *International Journal of Solids and Structures*, vol. 50, pp. 3829–3842, 24 2013.

[6] F. Pierron and M. Grédiac, "Towards material testing 2.0. a review of test design for identification of constitutive parameters from full-field measurements," *Strain*, vol. 57, 1 2021.

[7] M. A. Sutton, J. J. Orteu, and H. Schreier, *Image correlation for shape, motion and deformation measurements*. Springer US, 2009.

[8] A. Buljac *et al.*, "Digital volume correlation: Review of progress and challenges," *Experimental Mechanics*, vol. 58, pp. 661–708, 5 2018.

[9] P. Badel, K. Genovese, and S. Avril, "3d residual stress field in arteries: Novel inverse method based on optical full-field measurements," *Strain*, vol. 48, pp. 528–538, 6 2012.

[10] J. Li, X. Xie, G. Yang, B. Zhang, T. Siebert, and L. Yang, "Whole-field thickness strain measurement using multiple camera digital image correlation system," *Optics and Lasers in Engineering*, vol. 90, pp. 19–25, 2017.

[11] K. Genovese, L. Cortese, M. Rossi, and D. Amodio, "A 360-deg digital image correlation system for materials testing," *Optics and Lasers in Engineering*, vol. 82, pp. 127–134, 2016.

[12] M. Rossi, L. Cortese, K. Genovese, A. Lattanzi, F. Nalli, and F. Pierron, "Evaluation of volume deformation from surface dic measurement," *Experimental Mechanics*, vol. 58, pp. 1181–1194, 7 2018.

[13] P. Lava, S. Cooreman, S. Coppieters, M. D. Strycker, and D. Debruyne, "Assessment of measuring errors in dic using deformation fields generated by plastic fea," *Optics and Lasers in Engineering*, vol. 47, pp. 747–753, 7-8 2009.

[14] R. Balcaen, L. Wittevrongel, P. L. Reu, P. Lava, and D. Debruyne, "Stereo-dic calibration and speckle image generator based on fe formulations," *Experimental Mechanics*, vol. 57, pp. 703–718, 5 2017.

[15] R. Balcaen, P. L. Reu, P. Lava, and D. Debruyne, "Stereo-dic uncertainty quantification based on simulated images," *Experimental Mechanics*, vol. 57, pp. 939–951, 6 2017.

[16] MatchID, *Matchid*, Available: http://www.matchid.eu/.